Electronic Supplementary Material (ESI) for Materials Horizons.
This journal is © The Royal Society of Chemistry 2022

Supporting Information

Dipole Moment Engineering Enables Universal B–N-Embedded Bipolar Hosts for OLEDs: An Old Dog Learns a New Trick

Shuang He, Junjie Liu, Ge Yang, Zhengyang Bin and Jingsong You**

Key Laboratory of Green Chemistry and Technology of Ministry of Education,

College of Chemistry, Sichuan University, 29 Wangjiang Road, Chengdu 610064,

People's Republic of China

**Correspondence to: binzhengyang@scu.edu.cn; jsyou@scu.edu.cn*

Table of contents

I. General Remarks

Unless otherwise noted, all reactions were carried out using Schlenk techniques under a nitrogen atmosphere. All reagents were obtained from commercial suppliers and used without further purification. The solvents were dried and purified using an Innovative Technology PS-MD-5 Solvent Purification System.

NMR spectra were obtained on an Agilent 400-MR DD2 spectrometer. The ^{1}H NMR (400 MHz) chemical shifts were measured relative to $CDCl_3$ as the internal reference ($CDCl_3$: $\delta = 7.26$ ppm). The ^{13}C NMR (100 MHz) chemical shifts were given using $CDCl_3$ as the internal standard ($CDCl_3$: $\delta = 77.16$ ppm). The GC-MS analysis was performed with Shimadzu GCMS-QP2010 SE. High-resolution mass spectra (HRMS) were obtained with a Shimadzu LCMS-IT-TOF (ESI). X-Ray single-crystal diffraction data were collected on an Oxford Xcalibur E single crystal diffraction. UV-visible absorption spectra experiments were conducted on a HITACHI U-2910 spectrometer. Fluorescence spectra was collected on a Horiba Jobin Yvon-Edison Fluoromax-3 fluorescence spectrometer with a calibrated integrating sphere system. Phosphorescence spectra were collected on a HITACHI F-7100 fluorescence spectrophotometer. Thermogravimetric analysis (TGA) was carried out using DTG-60(H) at a rate of 10 °C/min under nitrogen atmosphere. Differential scanning calorimetry (DSC) thermogram was recorded on DSC 200PC equipment under nitrogen atmosphere at a rate of 10 °C/min. Cyclic voltammogram were performed on LK2005A with a solution of tetrabutylammonium hexafluorophosphate (Bu_4NPF_6, 0.1 M) in DCM as electrolyte and ferrocene/ferrocenium (Fc/Fc^+) as standard. Three-electrode system (Ag/Ag^+, platinum wire and glassy carbon electrode as reference, counter and work electrode respectively) was used in the CV measurement. AFM images were obtained by using a Bruker Inova atomic microscope in tapping mode.

II. OLED Fabrication and Characterization

Indium-tin-oxide (ITO) coated glass with a sheet resistance of 15 Ω sq^{-1} was used as the anode substrate. Prior to film deposition, patterned ITO substrates were cleaned with alkaline detergent, boiled deionized water, and deionized water thoroughly in ultrasonic bath, dried in an oven, and finally treated with oxygen plasma for 10 min to enhance the surface work function of ITO anode. All of the organic layers were deposited with the rate of 0.1 $\mathrm{nm{\cdot}s^{-1}}$ under high vacuum. The doped and co-doped layers were prepared by co-evaporating dopant and host material from two or three individual sources, and the doping concentrations were modulated by controlling the evaporation rates of dopant.

Current density-voltage-luminance characteristics were measured by using KEYSIGHT B1500A. The luminance and electroluminescence spectra were collected with model DLM-100Z photometer and OPT2000 spectrophotometer, respectively.

III. Synthesis and Characterization

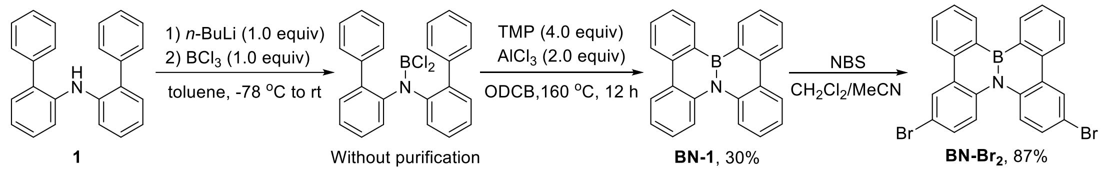

Scheme S1. Synthesis of **BN-1** and **BN-Br$_2$**.

Synthesis of 4b-aza-12b-boradibenzo[*g, p*]chrysene (BN-1)

4b-Aza-12b-boradibenzo[*g*,*p*]chrysene (**BN-1**) was prepared according to the literature procedures.[1] A solution of butyllithium in hexane (12 mL, 2.50 M, 30 mmol) was added slowly to a solution of **1** (9.64 g, 30 mmol) in toluene (150 mL) at –78 ºC under argon. After 1 h, the reaction mixture stirred at 0 ºC for 1 h. A solution of boron trichloride in hexane (30 mL, 1.0 M, 30 mmol) was added at –78 ºC. After stirring at room temperature for 8 h, the solvent was removed in vacuo, and another solvent of dry 1,2-dichlorobenzene (ODCB, 200 mL) was added. Aluminum trichloride (16 g, 120 mmol) and 2,2,6,6-tetramethylpiperidine (TMP, 8.5 g, 60 mmol) was added at 0 ºC, successively. After stirring at 160 ºC for 24 h, 1,4-diazabicyclo[2.2.2]octane (13.5 g, 120 mmol) was added. The reaction mixture was filtered with a pad of celite, and washed with dichloromethane (DCM). After the solvent was removed in vacuo, the crude product was purified by flash chromatography on silica gel (petroleum ether/DCM = 10/1, v/v) and following recrystallization from hexane/DCM afforded **BN-1** as a white solid (2.96 g, 30% yield). ^{1}H NMR (400 MHz, $CDCl_3$): δ = 7.32-7.40 (m, 4H), 7.62 (dt, *J* = 7.6 Hz, 0.8 Hz, 2H), 7.77-7.81 (m, 2H), 8.12 (dd, *J* = 8.0 Hz, 1.2 Hz, 2H), 8.37 (dd, *J* = 8.0 Hz, 1.6 Hz, 2H), 8.42 (d, *J* = 8.0 Hz, 2H), 8.70 (dd, *J* = 7.6 Hz, 1.2 Hz, 2H) ppm. ^{13}C NMR (100 MHz, $CDCl_3$): δ = 121.5, 123.2, 125.7, 126.91, 126.93, 127.7, 131.2, 135.7, 137.2, 139.0 ppm. Carbon adjacent to boron not observed. HRMS (ESI$^+$): calcd for $C_{24}H_{17}BN$ $[M+H]^+$ 330.1449; found 330.1452.

Synthesis of 2,7-dibromo-4b-aza-12b-boradibenzo[*g,p*]chrysene (BN-Br$_2$).

2,7-Dibromo-4b-aza-12b-boradibenzo[*g,p*]chrysene (**BN-Br$_2$**) was prepared according to the literature procedures.[2] To a solution of **BN-1** (3.29 g, 10 mmol) in DCM (120 mL) and MeCN (40 mL) at 0 °C was added *N*-bromosuccinimide (NBS) (3.56 g, 20 mmol) in portions. The ice bath was removed and the mixture was stirred at room temperature overnight. The reaction was quenched with water and extracted with DCM. The combined organic phase was dried over anhydrous Na_2SO_4. The solvent was removed under vacuum and the crude product was purified by column chromatography on silica gel (petroleum ether/DCM = 10:1, v/v) to afford compound **BN-Br$_2$** as a white solid (yield = 4.24 g, 87%). ^{1}H NMR (400 MHz, $CDCl_3$): δ =7.43 (dd, *J* = 9.2 Hz, 2.0 Hz, 2H), 7.64 (t, *J* = 7.6 Hz, 2H), 7.80 (t, *J* = 7.6 Hz, 2H), 7.85 (d, *J* = 8.8 Hz, 2H), 8.32 (d, *J* = 8.4 Hz, 2H), 8.44 (m, 2H), 8.65 (d, *J* = 7.6 Hz, 2H) ppm. ^{13}C NMR (100 MHz, $CDCl_3$): δ = 116.3, 122.9, 123.2, 127.6, 128.4, 129.6, 129.7, 131.6, 135.7, 135.8, 137.6 ppm. Carbon adjacent to boron not observed. HRMS (ESI$^+$): calcd for $C_{25}H_{17}BBr_2NO$ $[M+CH_3O]^-$, 517.9755 (100%), 515.9775 (51.4%), 519.9735 (48.6%); found 517.9761 (100%), 515.9791 (51.4%), 519.9738 (48.6%).

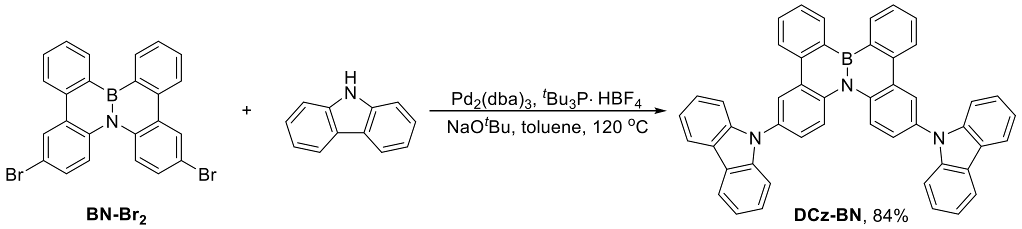

Scheme S2. Synthesis of **DCz-BN**.

Synthesis of 2,7-(9*H*-carbazol-9-yl)-4b-aza-12b-boradibenzo[*g,p*]chrysene (DCz-

BN).

An oven-dried Schlenk tube with a magnetic stir bar was charged with 2,7-dibromo-4b-aza-12b-boradibenzo[*g,p*]chrysene (**BN-Br$_2$**, 97.4 mg, 0.2 mmol), 9*H*-carbazole (**Cz**, 83.6 mg, 0.5 mmol, 2.5 equiv.), $Pd_2(dba)_3$ (9.2 mg, 0.01 mmol, 5 mol%), ^{t}Bu$_3$P•HBF$_4$ (11.6 mg, 0.04 mmol, 20 mol%), ^{t}BuONa (76.9 mg, 0.8 mmol, 4.0 equiv.) and toluene (2 mL) and stirred at 120 ^{o}C for 24 h under a nitrogen atmosphere. After cooling to room temperature, the reaction mixture was extracted with dichloromethane and brine, and dried over anhydrous Na_2SO_4. After filtration and evaporation, the crude product was purified by column chromatography on neutral alumina (200-300 mesh, petroleum ether/DCM = 10:1 to 4:1, v/v) and recrystallized from dichloromethane and methanol to afford **DCz-BN** as a white solid (yield = 110.7 mg, 84%). ^{1}H NMR (400 MHz, $CDCl_3$): δ = 7.34 (t, J = 7.6 Hz, 4H), 7.45-7.53 (m, 8H), 7.64-7.67 (dd, J = 8.8 Hz, 2.0 Hz, 2H), 7.70 (t, J = 7.2 Hz, 2H), 7.81 (t, J = 7.6 Hz, 2H), 8.21 (d, J = 7.6 Hz, 4H), 8.37 (d, J = 8.0 Hz, 2H), 8.48 (d, J = 8.8 Hz, 2H), 8.60 (d, J = 2.0 Hz, 2H), 8.80 (d, J = 7.6 Hz, 2H) ppm. ^{13}C NMR (100 MHz, $CDCl_3$): δ = 109.9, 120.1, 120.6, 123.0, 123.4, 123.5, 124.4, 125.9, 126.2, 127.7, 129.3, 131.7, 132.9, 135.9, 136.2, 138.3, 141.3 ppm. Carbon adjacent to boron not observed. HRMS (ESI$^+$): calcd for $C_{48}H_{31}BN_3$ $[M+H]^+$ 660.2606; found 660.2608.

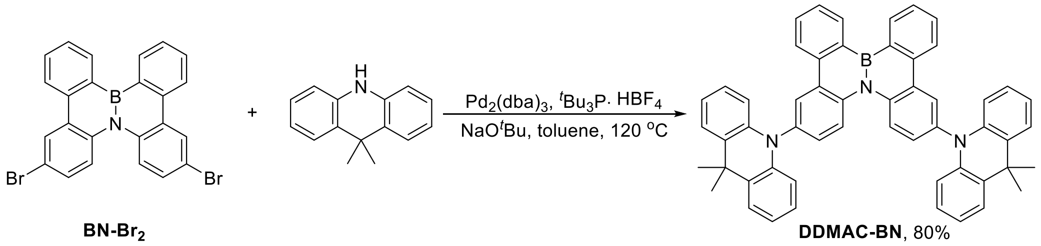

Scheme S3. Synthesis of **DDMAC-BN**.

Synthesis of 2,7-(9,9-dimethylacridin-10(9*H*)-yl)-4b-aza-12b-boradibenzo[*g,p*]chrysene (DDMAC-BN).

2,7-(9,9-Dimethylacridin-10(9*H*)-yl)-4b-aza-12b-boradibenzo[*g,p*]chrysene (**DDMAC-BN**) was synthesized according to the same procedure described above for the synthesis of **DCz-BN**, using **BN-Br$_2$** (97.4 mg, 0.2 mmol) and 9,9-dimethyl-9,10-dihydroacridine (**DMAC**, 104.7 mg, 0.5 mmol, 2.5 equiv.). **DDMAC-BN** was afforded as a white solid (yield = 118.9 mg, 80%). ^{1}H NMR (400 MHz, $CDCl_3$): δ = 1.78 (s, 12H), 6.48 (dd, J = 8.0 Hz, 1.6 Hz, 4H), 6.95-7.00 (m, 8H), 7.43 (dd, J = 8.8 Hz, 2.4 Hz, 2H), 7.52 (dd, J = 7.6 Hz, 1.6 Hz, 4H), 7.69 (t, J = 7.2 Hz, 2H), 7.80 (t, J = 8.0 Hz, 2H), 8.36 (d, J = 8.0 Hz, 2H), 8.40 (d, J = 2.4 Hz, 2H), 8.52 (d, J = 8.8 Hz, 2H), 8.79 (d, J = 7.2 Hz, 2H) ppm. ^{13}C NMR (100 MHz, $CDCl_3$): 31.6, 36.2, 114.3, 120.8, 123.5, 124.0, 125.5, 126.6, 127.6, 128.6, 129.8, 130.2, 130.3, 131.6, 135.9, 136.3, 136.7, 138.3, 141.2 ppm. Carbon adjacent to boron not observed. HRMS (ESI^{+}): calcd for $C_{54}H_{43}BN_3$ $[M+H]^{+}$ 744.3545, found 744.3551.

IV. Method of Theoretical Calculations

All theoretical calculations were performed using Gaussian 09[3] serials software. The ground-state structures and the energy levels and distributions of frontier molecular orbital were obtained by B3LYP[4] density functional method with basis set 6-31G*. The triplet spin density distributions were calculated by time-dependent DFT (TD-DFT) method with the same parameters for ground-state calculations. The frontier molecular orbital and triplet spin density distributions were visualized using Gaussview 5.0 software.

V. Crystal Data

Table S1. Crystal Data for **DCz-BN** [CCDC 2157582]

Identification code	**DCz-BN**
Empirical formula	$C_{48}H_{30}BN_3$
Formula weight	659.56
Temperature/K	151.0
Crystal system	monoclinic
Space group	$P2_1/c$
a/Å	14.234(2)
b/Å	19.457(3)
c/Å	12.568(2)
α/°	90
β/°	100.195(7)
γ/°	90
Volume/Å^3	3425.9(9)
Z	4
ρ_{calc}g/cm^3	1.279
μ/mm^{-1}	0.074
F(000)	1376.0
Crystal size/mm^3	0.16 × 0.15 × 0.05
Radiation	MoKα (λ = 0.71073)
2Θ range for data collection/°	3.902 to 55.016
Index ranges	$-18 \leq h \leq 18$, $-25 \leq k \leq 24$, $-16 \leq l \leq 15$
Reflections collected	23395
Independent reflections	7804 [R_{int} = 0.0583, R_{sigma} = 0.0652]
Data/restraints/parameters	7804/0/469
Goodness-of-fit on F^2	1.026
Final R indexes [I>=2σ (I)]	R1 = 0.0503, wR2 = 0.1126
Final R indexes [all data]	R1 = 0.0749, wR2 = 0.1277
Largest diff. peak/hole / e Å^{-3}	0.33/-0.23

Table S2. Crystal Data for **DDMAC-BN** [CCDC 2157583]

Identification code	**DDMAC-BN**
Empirical formula	$C_{54}H_{42}BN_3$
Formula weight	743.71
Temperature/K	302.0
Crystal system	monoclinic
Space group	C2/c
a/Å	27.5838(11)
b/Å	9.1201(4)
c/Å	19.3361(9)
α/°	90
β/°	124.5860(10)
γ/°	90
Volume/Å^3	4004.7(3)
Z	4
ρ_{calc}g/cm^3	1.234
μ/mm^{-1}	0.071
F(000)	1568.0
Crystal size/mm^3	0.42 × 0.31 × 0.21
Radiation	MoKα (λ = 0.71073)
2Θ range for data collection/°	4.814 to 55.046
Index ranges	$-32 \leq h \leq 35$, $-11 \leq k \leq 11$, $-25 \leq l \leq 25$
Reflections collected	34785
Independent reflections	4587 [R_{int} = 0.0791, R_{sigma} = 0.0513]
Data/restraints/parameters	4587/0/266
Goodness-of-fit on F^2	1.029
Final R indexes [I>=2σ (I)]	R1 = 0.0460, wR2 = 0.0994
Final R indexes [all data]	R1 = 0.0946, wR2 = 0.1185
Largest diff. peak/hole / e Å^{-3}	0.18/-0.14

VI. Additional Spectra and Data

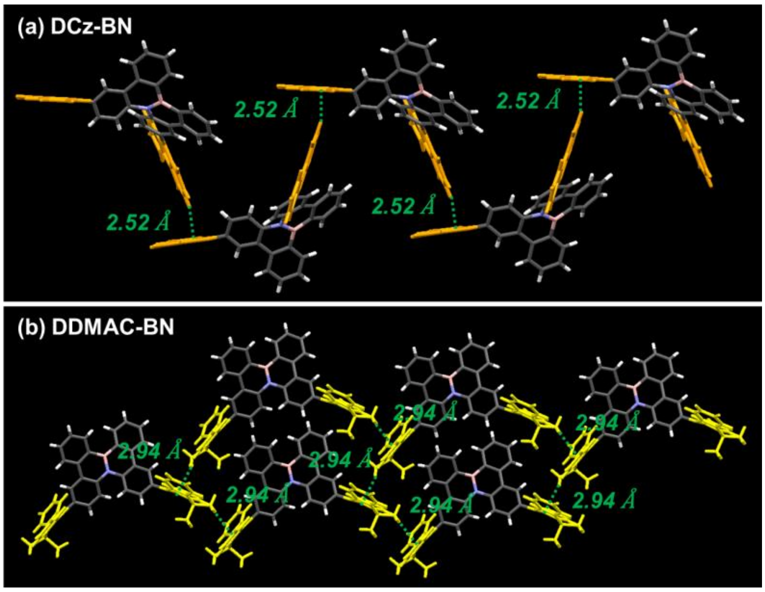

Fig. S1 Packing patterns with weak C−H···π interactions between the donors of (a) **DCz-BN** and (b) **DDMAC-BN**.

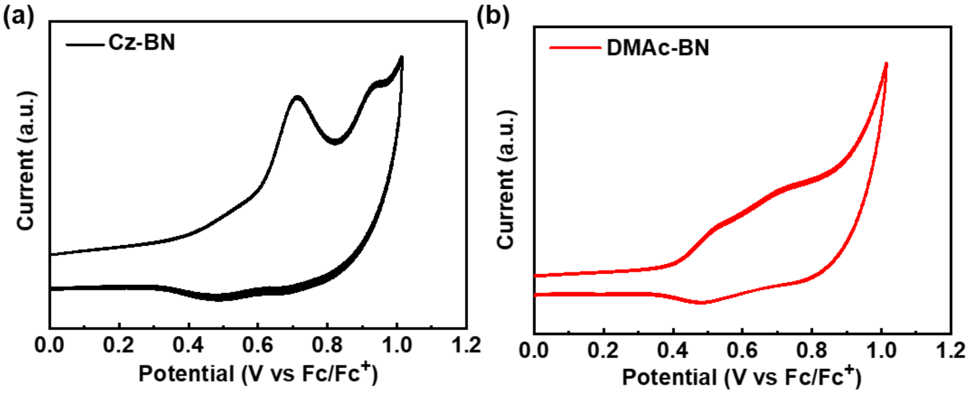

Fig. S2 Cyclic voltammograms of (a) **DCz-BN** and (b) **DDMAC-BN** measured in dry dichloromethane containing 0.1 M of tetrabutylammonium hexafluorophosphate.

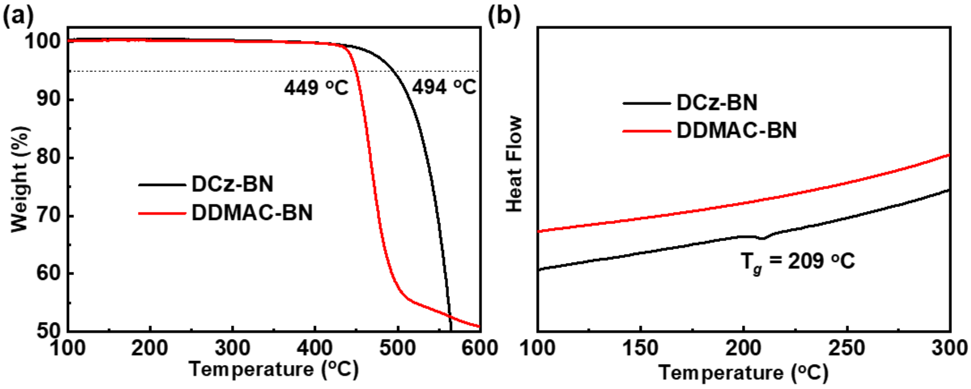

Fig. S3 (a) TGA curves of **DCz-BN** and **DDMAC-BN**. (b) DSC thermograms of **DCz-BN** and **DDMAC-BN**.

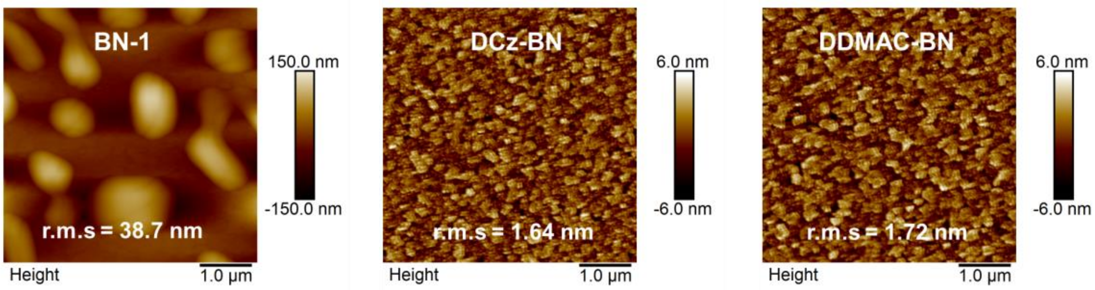

Fig. S4 Morphologies of **DCz-BN**, **DDMAC-BN** and **BN-1** films with the root-mean-square (r.m.s) values measured by atomic force microscope (AFM) after being heated at the temperature of 80 °C for 1 h.

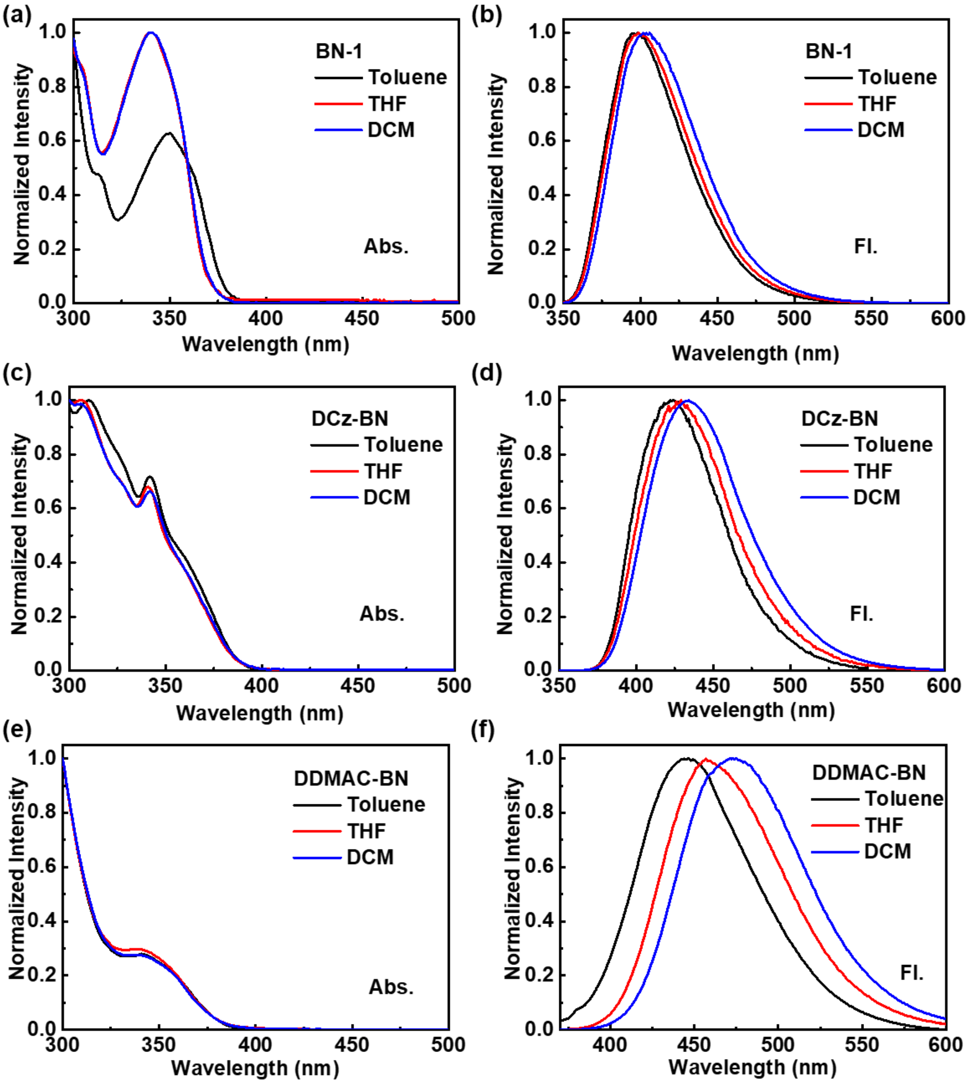

Fig. S5 Absorption spectra (Abs.) and fluorescence spectra (Fl.) of **BN-1**, **DCz-BN**, and **DDMAC-BN** measured in the solvents with different polarities.

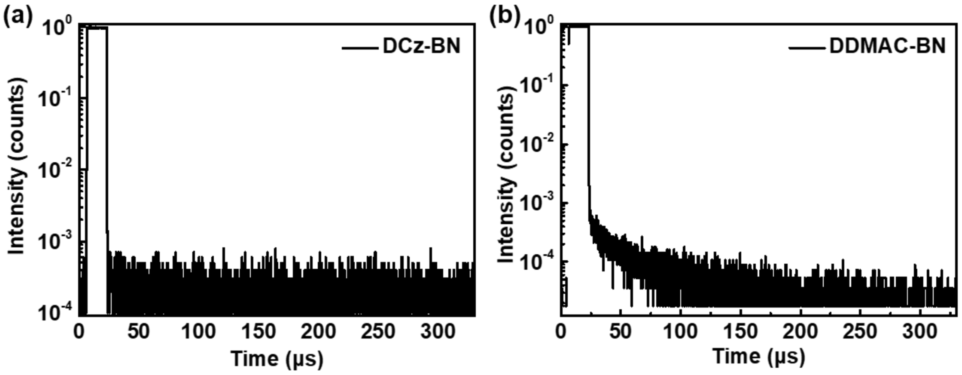

Fig. S6 Transient photoluminescence spectra of the 20 wt% **DCz-BN**- and **DDMAC-BN**-doped **DPEPO** films.

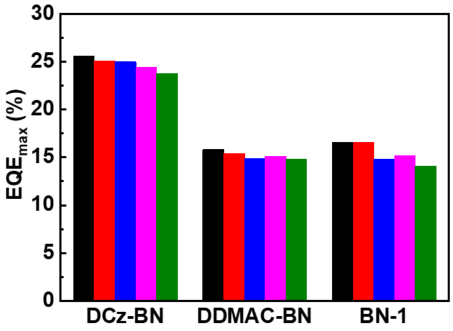

Fig. S7 EQE$_{max}$ distributions and statistics of **DACT-II**-based OLEDs.

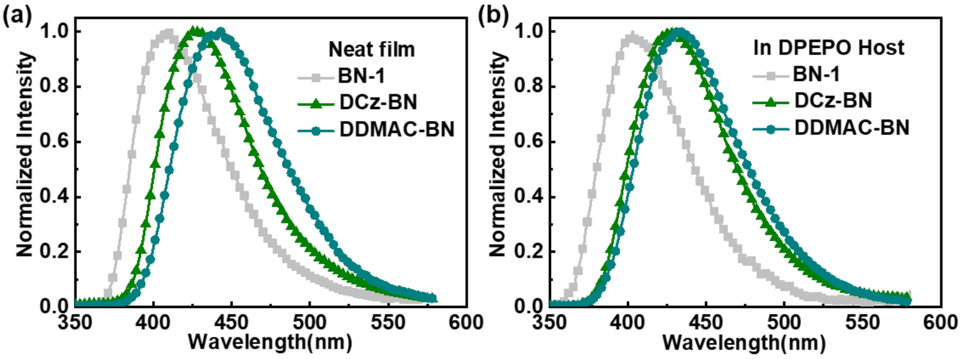

Fig. S8 Fluorescence spectra of (a) the neat films and (b) the 20 wt% doped **DPEPO** films of **BN-1**, **DCz-BN** and **DDMAC-BN**.

Table S3. Summary of thermal, electrochemical and photophysical properties.

Compound	T_d [°C]	T_g [°C]	HOMO[a] [eV]	LUMO[b] [eV]	λ_{abs}[c] [nm]
DCz-BN	494	209	-5.4	-2.2	309.8/341.2
DDMAC-BN	449	-	-5.2	-2.0	341.6
Compound	E_g[c] [eV]	λ_{em}[d] [nm]	E_{S1}[e] [eV]	E_{T1}[f] [eV]	ΔE_{ST}[g] [eV]
DCz-BN	3.20	423.4/429.1/429.2	3.28	2.93	0.35
DDMAC-BN	3.20	445.3/443.3/432.4	3.21	2.93	0.28

[a] Measured in dry dichloromethane solution (1×10^{-3} M) where $E_{HOMO} = -4.8 - (E_{ox} - E_{Fc})$. [b] Estimated according to the absorption spectrum and the HOMO energy level. [c] Calculated from the absorption spectrum. [d] Measured in toluene solution (1×10^{-5} M)/neat film/20 wt% doped **DPEPO** film at room temperature. [e] Estimated from the onset wavelength of fluorescence spectra measured in toluene solution (1×10^{-5} M) at 298 K. [f] Estimated from the onset wavelength of phosphorescence spectra measured in toluene solution (1×10^{-5} M) at 77 K. [g] Calculated from E_{S1} and E_{T1}.

Table S4: Summary of the optimized device structures.

Green TADF-OLEDs:
ITO/**TAPC** (30 nm)/**TCTA** (8 nm)/20% **DACT-II**: **DCz-BN** or **DDMAC-BN** or **BN-1** (25 nm)/**TmPyPb** (40 nm)/LiF (0.8 nm)/Al (100 nm)
Blue MR-OLEDs:
ITO/**TAPC** (30 nm)/**TCTA** (8 nm)/2% **BCz-BN**: **DCz-BN** (20 nm)/**PPF** (10 nm)/ **TmPyPb** (40 nm)/LiF (0.8 nm)/Al (100 nm)
Yellow TSF-OLEDs:
ITO/**TAPC** (30 nm)/**TCTA** (8 nm)/1% **TBRb**: 20% **DACT-II**: **DCz-BN** (30 nm)/ **TmPyPb** (40 nm)/LiF (0.8 nm)/Al (100 nm)
Red Ph-OLEDs:
ITO/**TAPC** (45 nm)/**TCTA** (8 nm)/2% **Ir(mphmq)$_2$(tmd)**: **DCz-BN** (20 nm)/ **TmPyPb** (45 nm)/LiF (0.8 nm)/Al (100 nm)

Table S5. Performance summary of **DACT-II**-based OLEDs (EQE$_{\text{max}}$ over 20%).

EML	V$_{\text{on}}$[a] [V]	V$_{1000}$[b] [V]	PE$_{\text{max}}$[c] [lm W^{-1}]	EQE$_{\text{max}}$[d] [%]	EQE$_{1000}$[e] [%]	EQE$_{5000}$[f] [%]	Ref.
DCz-BN: 20% DACT-II	2.9	4.4	83.0	25.6	23.6	18.7	This work
TCTA: B3PYMPM: 7% DACT-II	--	--	121.3	34.2	31.0	--	5
CBP: 9% DACT-II	--	--	--	29.6	20.4	--	6
32aICTRZ: 15% DACT-II	--	--	79.0	27.1	--	26.2	7
23aICTRZ: 15% DACT-II	--	--	-	24.2	--	21.2	7
23bICTRZ: 15% DACT-II	--	--	-	20.3	--	19.2	7
26DCzPPy: 15% DACT-II	--	--	43.1	23.9	--	19.7	7
DCzPPy: 20% DACT-II	3.2	--	61.3	26.1	--	--	8
***m*CBP: 15% DACT-II**				24.3		16.2	9
3Cz46Pm: 20% DACT-II	3.1		53.4	22.7		20.1	10
2Cz46Pm: 20% DACT-II	3.2		51.0	21.5		19.3	10
9Cz46Pm: 20% DACT-II	3.3		52.4	22.8		19.8	10
PhCz-*o*-Trz: 10% DACT-II	--	4.5	38.8	20.2	19.0	16.0	11

[a] Turn-on voltage at 1 cd m^{-2}. [b] Driving voltage at 1000 cd m^{-2}. [c] Maximum Power efficiency. [d] Maximum External quantum efficiency. [e] External quantum efficiency at 1000 cd m^{-2}. [f] External quantum efficiency at 5000 cd m^{-2}.

Table S6. Performance summary of **BCz-BN**-based OLEDs (EQE$_{max}$ over 20%).

EML	V$_{on}$[a] [V]	V$_{1000}$[b] [V]	PE$_{max}$[c] [lm W^{-1}]	EQE$_{max}$[d] [%]	EQE$_{1000}$[e] [%]	EQE$_{5000}$[f] [%]	Ref.
DCz-BN: 2% BCz-BN	2.9	4.2	37.1	21.7	10.5	5.9	This work
***m*CBP: 2% BCz-BN**	--	--	--	27.8	--	--	12
***m*CBP: 20% CTPCF3: 1% BCz-BN**	3.0	--	79.0	27.5	--	24.1	13
***m*CBP: 1% BCz-BN**	3.6	--	37.7	21.6	5.3	--	14

[a] Turn-on voltage at 1 cd m^{-2}. [b] Driving voltage at 1000 cd m^{-2}. [c] Maximum Power efficiency. [d] Maximum External quantum efficiency. [e] External quantum efficiency at 1000 cd m^{-2}. [f] External quantum efficiency at 5000 cd m^{-2}.

Table S7. Performance summary of **TBRb**-based OLEDs (EQE$_{max}$ over 20%).

EML	V$_{on}$[a] [V]	V$_{1000}$[b] [V]	PE$_{max}$[c] [lm W^{-1}]	EQE$_{max}$[d] [%]	EQE$_{1000}$[e] [%]	EQE$_{5000}$[f] [%]	Ref.
DCz-BN: 20% DACT-II: 1% TBRb	2.7	4.4	96.1	24.7	21.2	17.0	This work
dMeACRXTO: 20% DACT-II: 1% TBRb	2.7	--	118.2	32.3	23.5	18.9	15
8-MeACRXTO: 20% DACT-II: 1% TBRb	2.4	--	109.0	25.5	18.6	15.3	15
TCTA: B4PYMPM: 8% Ir(ppy)$_2$tmd: 2% TBRb	2.2	2.9	114.3	26.1	26.0	--	16
TCTA: B4PYMPM: 8% Ir(ppy)$_3$: 2% TBRb	2.3	3.1	100.4	25.0	24.8	--	16
***m*CBP: 20% 5Cz-TRZ: 1% TBRb**	--	--	--	24.9	--	--	9
SF4-TPE: 10% PXZ-TRZ: 1% TBRb	4.1	--	55.8	23.5	21.5	17.8	17
SF4-TPE: 20% PXZ-TRZ: 1% TBRb	3.9	--	61.6	24.7	23.6	20.7	17
SF4-TPE: 30% PXZ-TRZ: 1% TBRb	3.8	--	62.1	24.2	23.5	21.4	17
SF4-TPE: 40% PXZ-TRZ: 1% TBRb	3.7	--	60.3	23.0	22.9	21.0	17
32aICTRZ: 10% DACz-TAZTRZ: 0.5% TBRb	2.1	--	82.1	23.7	23.2	20.6	18
PhCzSPOTz: 3% TBRb	2.6	5.0	78.3	20.9	19.2	--	19

PVK: 20% CMA1: 2% TBRb	--	--	--	20.4	14.0	--	20
PBICT: 20% PyCNTruX: 0.5% TBRb	4.5	--	50.7	20.2	20.2	--	21

[a] Turn-on voltage at 1 cd m^{-2}. [b] Driving voltage at 1000 cd m^{-2}. [c] Maximum Power efficiency. [d] Maximum External quantum efficiency. [e] External quantum efficiency at 1000 cd m^{-2}. [f] External quantum efficiency at 5000 cd m^{-2}.

Table S8. Performance summary of **Ir(mphmq)$_2$(tmd)**-based OLEDs (EQE$_{max}$ over 20%).

EML	V$_{on}$[a] [V]	V$_{1000}$[b] [V]	PE$_{max}$[c] [lm W^{-1}]	EQE$_{max}$[d] [%]	EQE$_{1000}$[e] [%]	EQE$_{5000}$[f] [%]	Ref.
DCz-BN: 2% Ir(mphmq)$_2$(tmd)	3.0	5.0	45.4	25.5	22.1	19.8	This work
NPB: B3PYMPM: 3.5% Ir(mphmq)$_2$(tmd)	2.1		66.2	35.6	35.1		22
NPB: PO-T2T: 5% Ir(mphmq)$_2$(tmd)	1.9	3.3	62.6	34.1	32.4		23
DMAC-SFNP: 3% Ir(mphmq)$_2$(tmd)	2.5			32.2			24
DMAC-BP: 3% Ir(mphmq)$_2$(tmd)	2.7			21.2			24
MeCz-EtBP: Ir(mphmq)$_2$(tmd)	2.7		55.7	28.1	19.6	16.5	25
DMAC-EtBP: Ir(mphmq)$_2$(tmd)	2.7		42.7	24.0	20.3	17.9	25
6e: 3% Ir(mphmq)$_2$(tmd)	3.5		44.4	27.3	19.4	17.7	26
6d: 3% Ir(mphmq)$_2$(tmd)	3.5		39.8	22.6	15.2	11.8	26
SBFTrz: BPBPCz: 5% Ir(mphmq)$_2$(tmd)	3.4		32.7	26.2	23.2		27
Bebq$_2$: 3% Ir(mphmq)$_2$(tmd)	2.1	3.7	32.0	24.6			28
HT10: ET14: 2% Ir(mphmq)$_2$(tmd)			43.2	23.0	20.7		29
DMAC-DPS: 0.5% Ir(mphmq)$_2$(tmd)				22.4		19.6	30
BBPICT: 2% Ir(mphmq)$_2$(tmd)	2.6	4.6	29.6	20.9	19.7	--	31
BBPICT: 1% Ir(mphmq)$_2$(tmd)	2.6	4.6	28.8	20.0	19	--	31

[a] Turn-on voltage at 1 cd m^{-2}. [b] Driving voltage at 1000 cd m^{-2}. [c] Maximum Power efficiency. [d] Maximum External quantum efficiency. [e] External quantum efficiency at 1000 cd m^{-2}. [f] External quantum efficiency at 5000 cd m^{-2}.

VII. References

1. T. Hatakeyama, S. Hashimoto, S. Seki, M. Nakamura, *J. Am. Chem. Soc.* **2011**, *133*, 18614-18617.
2. S. Hashimoto, T. Ikuta, K. Shiren, S. Nakatsuka, J. Ni, M. Nakamura, T. Hatakeyama, *Chem. Mater.* **2014**, *26*, 6265-6271.
3. M. J. Frisch, G. W. Trucks, H. B. Schlegel, G. E. Scuseria, M. A. Robb, J. R. Cheeseman, G. Scalmani, V. Barone, B. Mennucci, G. A. Petersson, H. Nakatsuji, M. Caricato, X. Li, H. P. Hratchian, A. F. Izmaylov, J. Bloino, G. Zheng, J. L. Sonnenberg, M. Hada, M. Ehara, K. Toyota, R. Fukuda, J. Hasegawa, M. Ishida, T. Nakajima, Y. Honda, O. Kitao, H. Nakai, T. Vreven, J. A. Jr. Montgomery, J. E. Peralta, F. Ogliaro, M. Bearpark, J. J. Heyd, E. Brothers, K. N. Kudin, V. N. Staroverov, R. Kobayashi, J. Normand, K. Raghavachari, A. Rendell, J. C. Burant, S. S. Iyengar, J. Tomasi, M. Cossi, N. Rega, N. J. Millam, M. Klene, J. E. Knox, J. B. Cross, V. Bakken, C. Adamo, J. Jaramillo, R. Gomperts, R. E. Stratmann, O. Yazyev, A. J. Austin, R. Cammi, C. Pomelli, J. W. Ochterski, R. L. Martin, K. Morokuma, V. G. Zakrzewski, G. A. Voth, P. Salvador, J. J. Dannenberg, S. Dapprich, A. D. Daniels, Ö. Farkas, J. B. Foresman, J. V. Ortiz, J. Cioslowski, D. J. Fox, Gaussian 09, Revision D.01, Gaussian, Inc., Wallingford CT, 2009.
4. a) A. D. Becke, *J. Chem. Phys.* **1993**, *98*, 5648-5652; b) C. Lee, W. Yang, R. G. Parr, *Phys. Rev. B.* **1988**, *37*, 785-789.
5. C.-K. Moon, K. Suzuki, K. Shizu, C. Adachi, H. Kaji, J.-J. Kim, *Adv. Mater.* **2017**, *29*, 1606448.
6. H. Kaji, H. Suzuki, T. Fukushima, K. Shizu, K. Suzuki, S. Kubo, T. Komino, H. Oiwa, F. Suzuki, A. Wakamiya, Y. Murata, C. Adachi, *Nat. Commun*. **2015**, *6*, 8476.
7. D. Zhang, X. Song, M. Cai, H. Kaji, Lian Duan, *Adv. Mater.* **2018**, *30*, 1705406.
8. K.-W. Tsai, M.-K. Hung, Y.-H. Mao, S.-A. Chen, *Adv. Funct. Mater*. **2019**, *29*, 1901025.
9. L.-S. Cui, Al. J. Gillett, S.-F. Zhang, H. Ye, Y. Liu, X.-K. Chen, Z.-S. Lin, E. W. Evans, W. K. Myers, T. K. Ronson, H. Nakanotani, S. Reineke, J.-L. Bredas, C.

Adachi, R. H. Friend, *Nat. Photonics* **2020**, *14*, 636-642.

10. M. Cai, D. Zhang, J. Xu, X. Hong, C. Zhao, X. Song, Y. Qiu, H. Kaji, L. Duan, *ACS Appl. Mater. Interfaces* **2019**, *11*, 1096-1108.
11. D. Zhang, K. Suzuki, X. Song, Y. Wada, S. Kubo, L. Duan, H. Kaji, *ACS Appl. Mater. Interfaces* **2019**, *11*, 7192-7198.
12. M. Yang, I. S. Park, T. Yasuda, *J. Am. Chem. Soc*. **2020**, *142*, 19468-19472.
13. Y. Zhang, J. Wei, D. Zhang, C. Yin, G. Li, Z. Liu, X. Jia, J. Qiao, L. Duan, *Angew. Chem. Int. Ed*. **2022**, *61*, e202113206.
14. Y. Xu, Z. Cheng, Z. Li, B. Liang, J. Wang, J. Wei, Z. Zhang, Y. Wang, *Adv. Optical Mater.* **2020**, *8*, 1902142.
15. Y. Ran, G. Yang, Y. Liu, W. Han, G. Gao, R. Su, Z. Bin, J. You, *Mater. Horiz.* **2021**, *8*, 2025-2031.
16. H.-G. Kim, K.-H. Kim, J.-J. Kim, *Adv. Mater*. **2017**, *29*, 1702159.
17. X. Tang, Y. Li, Y.-K. Qu, C.-C. Peng, A. Khan, Z.-Q. Jiang, L.-S. Liao, *Adv. Funct. Mater*. **2020**, *30*, 1910633.
18. R. Su, Y. Zhao, F. Yang, L. Duan, J. Lan, Z. Bin, J. You, *Sci. Bull.*, **2021**, *5*, 441-448.
19. C. Duan, Y. Xin, Z. Wang, J. Zhang, C. Han, H. Xu, *Chem. Sci.*, **2022**, *13*, 159-169.
20. L. Yang, V. Kim, Y. Lian, B. Zhao, D. Di, *Joule* **2019**, *3*, 2381-2389.
21. J. H. Kim, K. H. Lee, J. Y. Lee, *J. Mater. Chem. C*, **2020**, *8*, 5265-5272.
22. K.-H. Kim, S. Lee, C.-K. Moon, S.-Y. Kim, Y.-S. Park, J.-H. Lee, J. W. Lee, J. Huh, Y. You, J.-J. Kim, *Nat. Commun*. **2014**, *5*, 4769.
23. J.-H. Lee, H. Shin, J.-M. Kim, K.-H. Kim, J.-J. Kim, *ACS Appl. Mater. Interfaces,* **2017**, *9*, 3277-3281.
24. W. Liang, Y. Yang, M. Yang, M. Zhang, C. Li, Y. Ran, J. Lan, Z. Bin, J. You, *Angew. Chem. Int. Ed*. **2021**, *60*, 3493-3497; *Angew. Chem*. **2021**, *133*, 3535-3539.
25. W. Ma, Z. Bin, G. Yang, J. Liu, J. You, *Angew. Chem. Int. Ed.* **2022**, *61*, e202116681; *Angew. Chem*. **2022**, *134*, e202116681.
26. Y. Luo, Z. Liu, G.Yang, T. Wang, Z. Bin, J. Lan, D. Wu, J. You, *Angew. Chem. Int.*

Ed. **2021**, *60*, 18852-18859; *Angew. Chem*. **2021**, *133*, 19000-19007.

27. V. V. Patil, J. Lim, J. Y. Lee, *Dyes Pigments*, **2021**, *189*, 109247.
28. D. H. Kim, N. S. Cho, H.-Y. Oh, J. H. Yang, W. S. Jeon, J. S. Park, M. C. Suh, J. H. Kwon, *Adv. Mater.* **2011**, *23*, 2721-2726.
29. C. Huang, Y. Zhang, J. Zhou, S. Sun, W. Luo, W. He, J. Wang, X. Shi, M.-K. Fung, *Adv. Optical Mater.* **2020**, *8*, 2000727.
30. P. Wei, D. Zhang, M. Cai, X. Song, Z. Wang, L. Duan, *Org. Electron.* **2017**, *49*, 242-248.
31. Y. Li, D. Zhang, L. Duan, *Org. Electron.* **2018**, *57*, 53-59.

VIII. Copies of NMR spectra

^{1}H NMR spectrum of **BN-1** (CDCl$_3$)

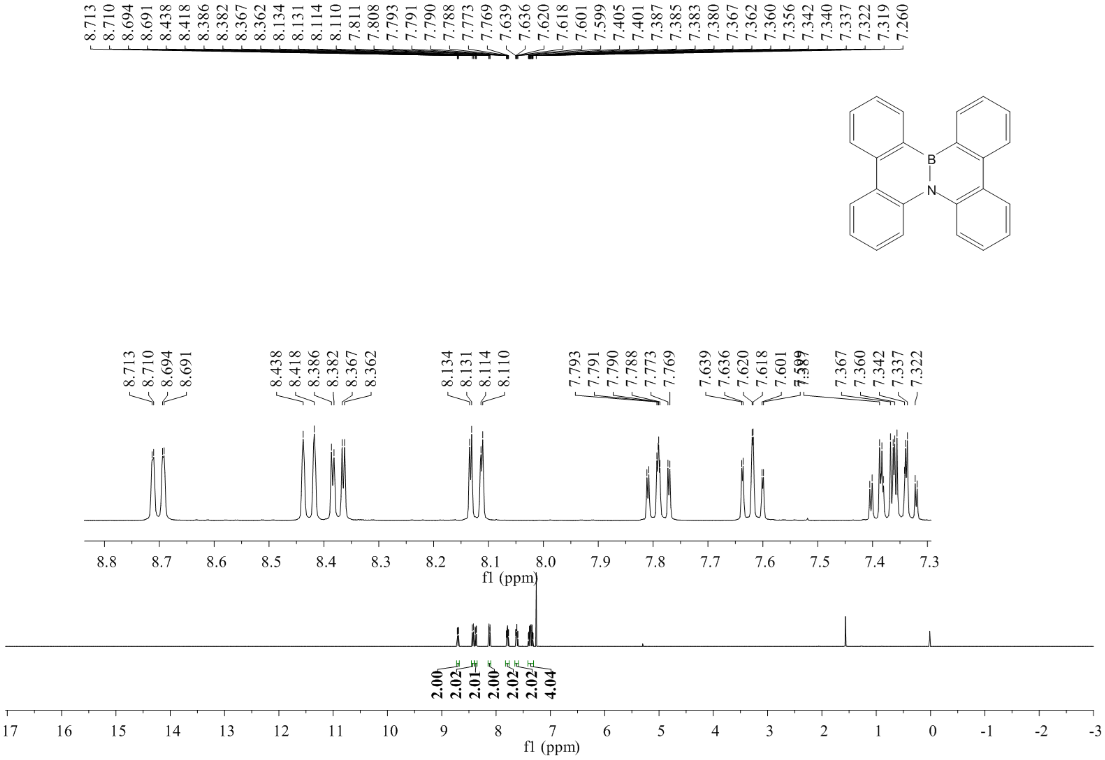

^{13}C NMR spectrum of **BN-1** (CDCl$_3$)

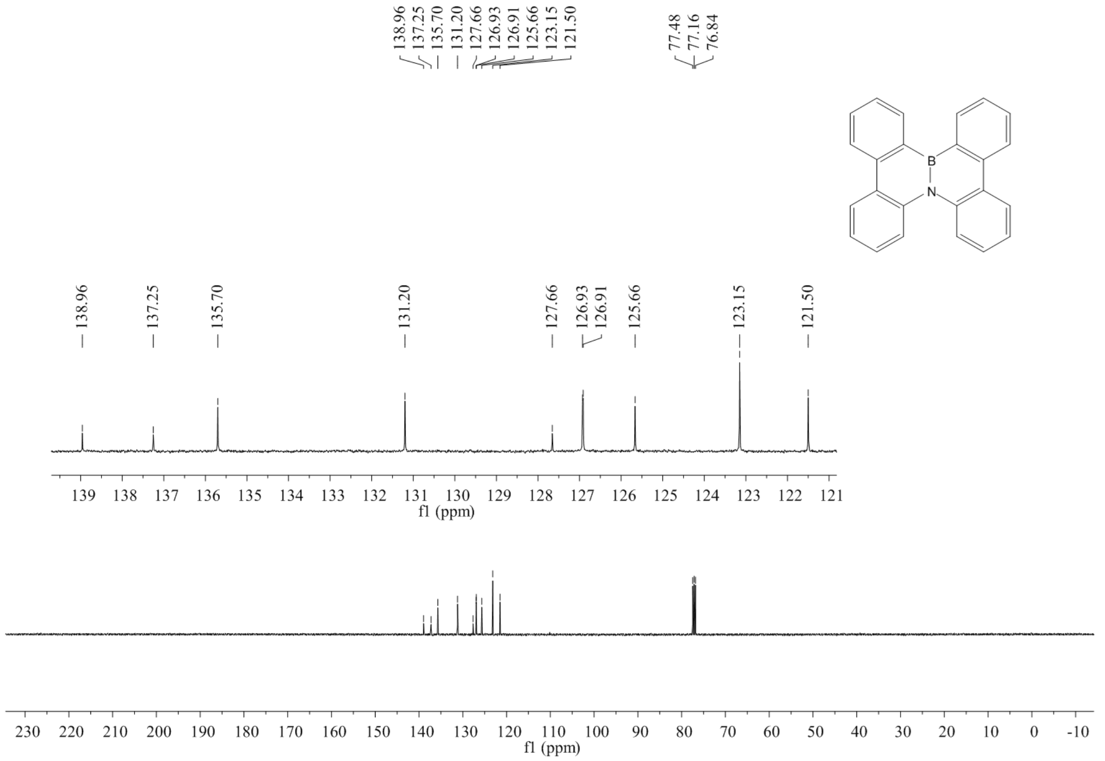

^{1}H NMR spectrum of **BN-Br$_2$** ($CDCl_3$)

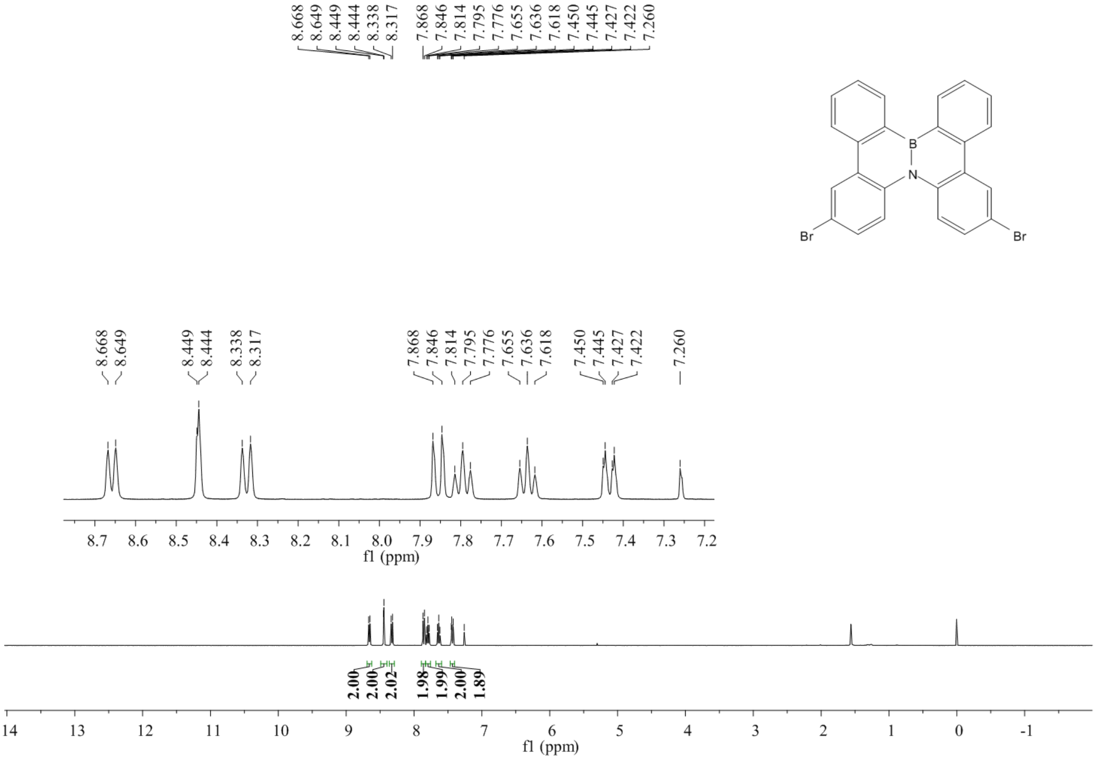

^{13}C NMR spectrum of **BN-Br$_2$** ($CDCl_3$)

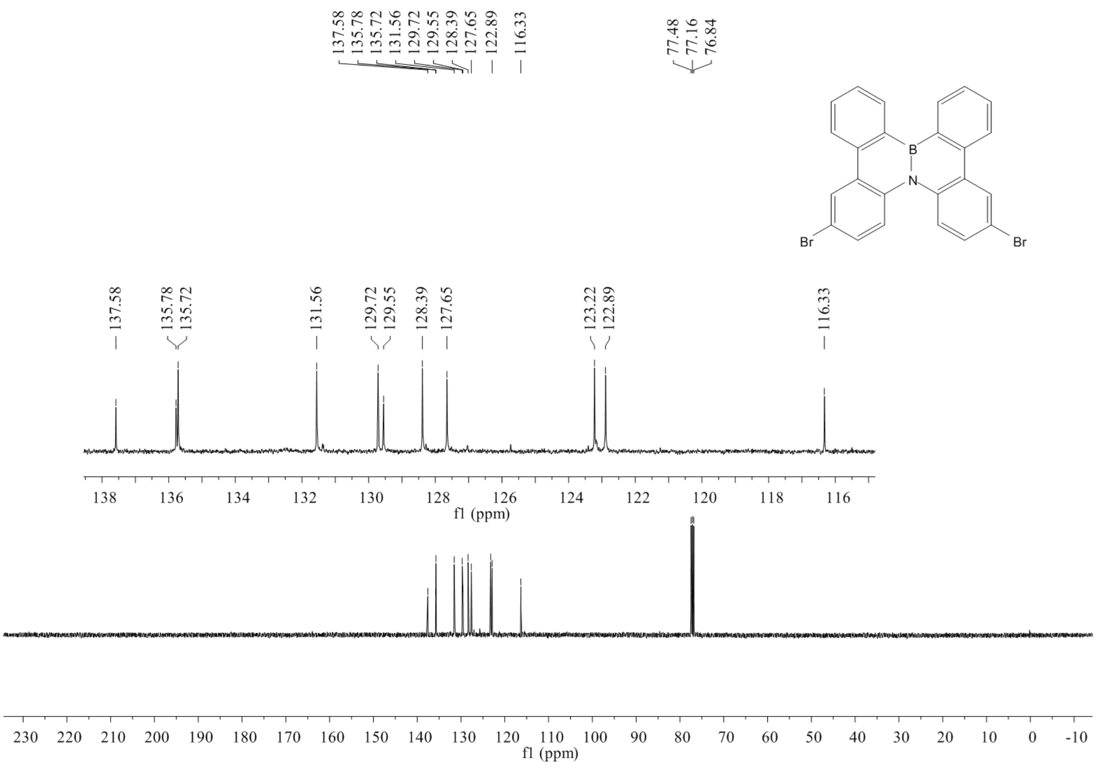

^{1}H NMR spectrum of **DCz-BN** ($CDCl_3$)

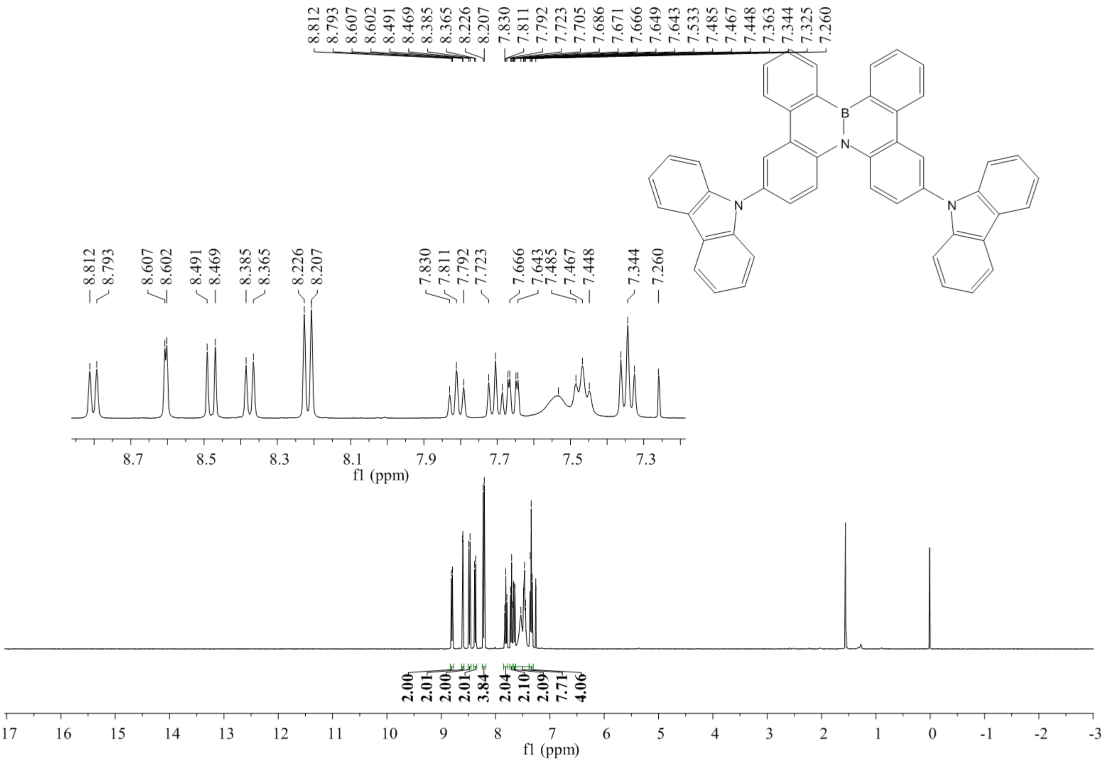

^{13}C NMR spectrum of **DCz-BN** ($CDCl_3$)

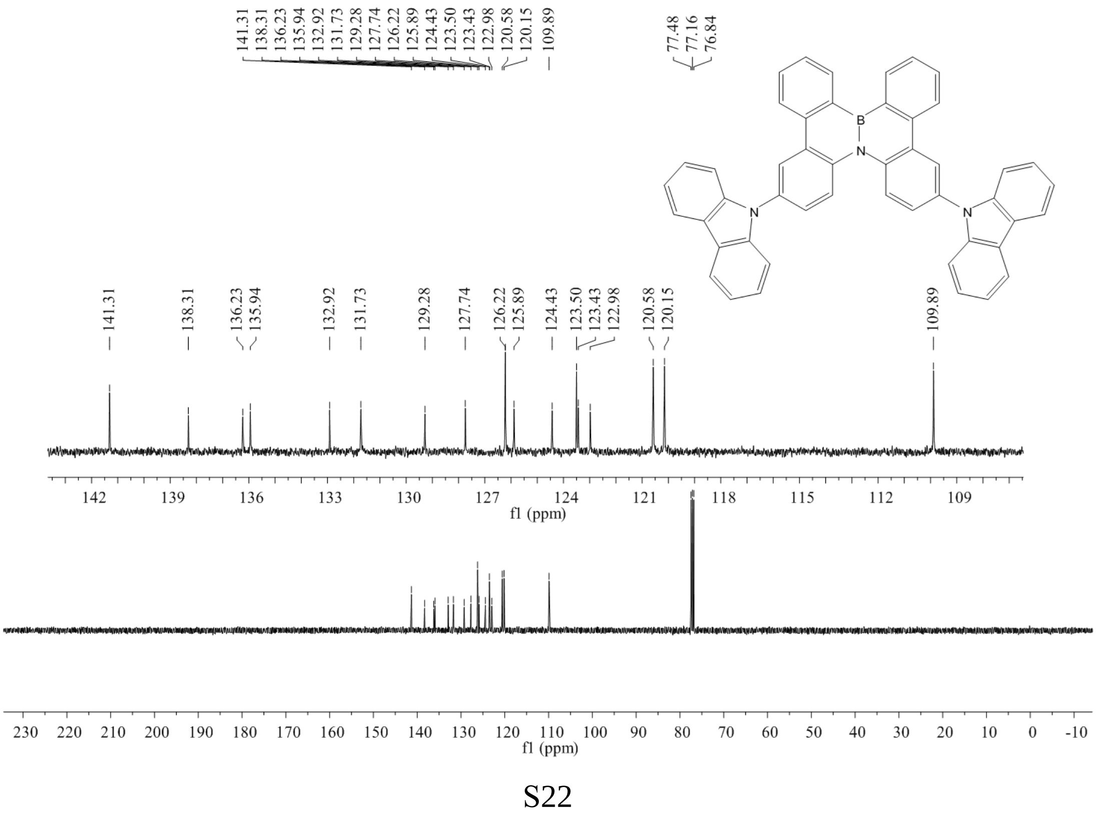

^1H NMR spectrum of **DDMAC-BN** ($CDCl_3$)

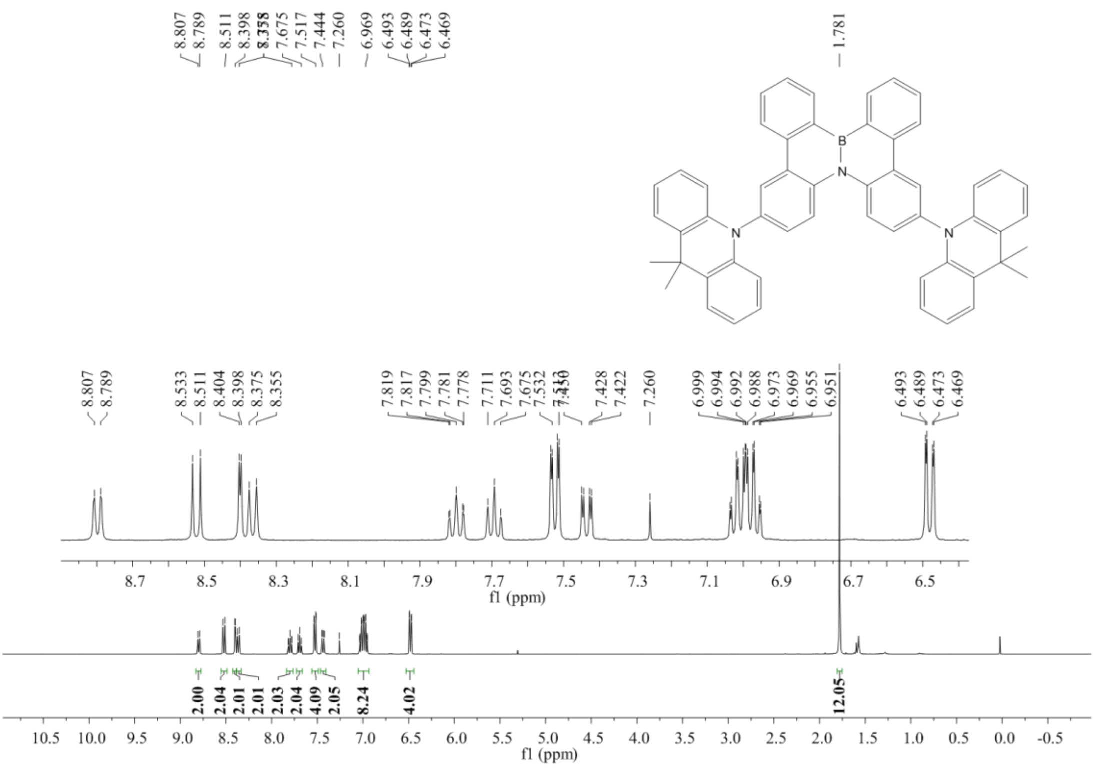

^{13}C NMR spectrum of **DDMAC-BN** ($CDCl_3$)